Design and Testing of Recycled 3D Printed Foldable Unmanned Aerial Vehicle for Remote Sensing

Jason Niemand [1], Sajith J Mathew [2], Felipe Gonzalez [3]

***Abstract*- Substantial progress in battery and control technology has drastically enabled unmanned aerial vehicles (UAVs) to evolve and develop for utilization across a broader array of applications. Remote sensing imagery in UAVs are evidently exhibiting its remarkable reliability, efficiency and integrability. Furthermore, technological advancements in additive manufacturing enable rapid prototyping of designs in a more cost-effective manner. This paper describes the design, construction and testing of a UAV with a foldable airframe, manufactured from recycled Polyethylene Terephthalate (PET) plastic, through 3D printing filament for the purpose of remote sensing. Previous contributions demonstrated the ability of manufacturing UAVs from recycled plastic and the feasibility of utilizing PET. This paper further develops the design, functionality and application of the UAV through additional material testing, design optimization and added design features. The new UAV design features include; propeller protection to enable remote sensing in isolated and inaccessible areas, integrated printed circuit board (PCB) to power onboard systems and reduce cable clutter, and material testing and analysis for usability of PET in multiple extreme weather environments. Moreover, the optimized UAV design will allow ease of integration with onboard systems, as well as cater for multiple interchangeable rotor arm designs, including protected and unprotected propeller designs. The objective of the research and investigation is focused on the development and implementation of cost-effective and environmentally sustainable UAVs. This paper strives to enable UAV manufacturers to rapidly prototype and optimize UAV designs, while simultaneously deterring PET plastic pollution globally, with negligible effect on UAV functionality.**

I. INTRODUCTION

A drastic growth for the design and demand of Unmanned Aerial Vehicles (UAVs and Drones) has been observed [1-7]. With UAVs becoming more compact, portable and adaptable, its popularity has increased, accommodating a broader spectrum of applications, such as; Search and Rescue, Traffic and Weather monitoring, Photography and more. The anticipated demand for UAVs is projected to reach $25 Billion USD by 2023, with a staggering growth rate of 18.2%.

Additive manufacturing, or 3D printing has greatly impacted the UAV industry through enabling the ability of rapid prototyping and design optimisation. With advantageous characteristics that supports the growing UAV industry, offering increased production efficiencies and ease of customizability. Nonetheless, producing a larger sum of parts within a decreased time period while utilizing standard printing filaments poses a severe projected environmental impact.

This paper's main objective aims to converse and understand the obstacles encountered throughout the design, construction and testing of the recycled 3D printed, foldable UAV, with an integrated air quality sensing system. This paper details the design, manufacturing, testing and verification of a more cost-effective, environmentally sustainable UAV design, featuring remote air quality sensing.

II. BACKGROUND

A. UAV Multirotor - Quadcopter

Quadcopters operate through the use of four motors, equally situated from the COG (Centre of Gravity). Two motors rotate in the clockwise motion and the other two in the anti-clockwise motion, thus bring the UAV into angular equilibrium.

To achieve successful flight of the recycled 3D printed UAV, a number of crucial components are required. For flight, four motors are essential to provide the airframe and onboard components with sufficient thrust. The required thrust can be determined through summing the total weight of the UAV, doubling the summed weight, and then adding an additional 20% of the doubled weight. The total can then be divided by the number of motors to determine the required thrust per motor [8]. Considering the kV rating of the motor is important when selecting motors for the purpose of the UAV. Ensuring motor efficiency is adequate, as this will conversely affect the life of battery power supply. Battery life can be estimated by dividing the thrust (in grams) by the power (in

[1] Jason Niemand is with the Queensland University of Technology, 2 George Street, Brisbane City, QLD, 4000. Contact: +61 422 109 649; (e-mail: jason.neimand@connect.qut.edu.au).

[2] Sajith J Mathew is with Queensland University of Technology, 2 George Street, Brisbane City, QLD, 4000. Contact: (e-mail: sajithjmathew@gmail.com).

[3] Felipe Gonzalez is with the Queensland University of Technology, 2 George Street, Brisbane City, QLD, 4000. Contact: +61 7 3138 1363; (e-mail: felipe.gonzalez@qut.edu.au).

Watts) of the motor. The C-rating is very important in selecting a battery in order to generate sufficient power and not negatively affect the overall weight of the UAV. ESCs (Electronic Speed Controllers) are vital devices that regulate the power of the motors through a microprocessor that drives a couple of FETs' (Field Effect Transistors) to generate a three phase AC current, enabling the motors to rotate at various throttle positions [9], [10].
The throttle positions are communicated to the ESCs from the RC transmitter to the receiver via the corresponding radio frequency. A camera and microcontroller are essential to achieve the remote sensing capability of the UAV. Subsequently, sufficient power must be supplied to all sources in order to function adequately.

B. Additive Manufacturing – 3D Printing

Additive manufacturing, or more commonly 3D printing is a process that involves the deposition of successive layers of suitable materials through a heated nozzle head to fabricate objects [11]. Layers can range from 16 to 180 microns, and occasionally thicker [12]. The 3D printing procedure comprises of a computer with 3D CAD modelling software. The 3D model is converted to an STL (Standard Triangle Language) format that describes the geometry of three-dimensional objects [13]. STL files utilize a string of triangles to embody a modelled object in CAD. Following a process known as 'Slicing' the 3D model is converted to G-Code [14]. Achieving the appropriate tolerance is crucial, as this can either lead to poor resolution and unnecessary file size increase.

C. Recycled Printing Filament – PET (Polyethylene Terephthalate)

In additive manufacturing, selecting the appropriate material to be utilized for construction of a prototype, is crucial to ensure the desired material properties is present. An endless range of filaments are available to suite a vast array of applications [15]. Filament options ranges from standard types, such as acrylonitrile butadiene styrene (ABS), to flexible options including thermoplastic polyurethane (TPU), and other composite materials.

PET filament will be utilized for the production of the UAV. PET is commonly used to manufacture water bottle and food containers. Demonstrating excellent material properties, PET is a hard, shockproof material, and is considered ideal for lightweight applications. The PET filament to be utilized in this project is provided by B-PET and is extracted directly from plastic bottle waste, which allows the repurposing of plastic waste and subsequently reduces the detrimental effects to the environment.

D. Remote Sensing – Air Quality Sensing

Remote sensing has become an increasingly popular method of acquiring various types of data, thus allowing our understanding of the environment, space and air to be greatly advanced [21]. With the abundance of sensors available, such as; air quality sensors, plant health sensors and Lidar cameras. Furthermore, these sensors can be integrated onto a UAV in order to capture meaningful data that can be interpreted for future treatment and/or solutions. The papers below were investigated to provide initiative for integrating an air quality sensor onto a UAV in order to record air quality samples for analysis.

Niethammer *et al.* [22] utilized UAVs with integrated cameras of compact size in order to monitor and map landslides at a rapidly increasing rate, with high resolution. An ortho-mosaic, high resolution image of the Super Sauze landslide in France was captured. Additionally, digital terrain models (DTMs) of numerous other regions. Further imagery of the area was taken over certain time period. The collected data was analysed, and persistent deformation was recorded. This study shows that remote sensing can be utilized to monitor and predict possible future landslides, thus measures of mitigating such events can be implemented.

Nebiker *et al.* [23] studied the effects of developing and successfully implementing a light-weight multi-spectral camera onto a micro UAV. The study consisted of collecting significant amounts of data to monitor the health of plants based on the percentage of damaged leaves. The procedure consisted of extracting raw imagery data from the sensors, then geo-referencing, corrections and masking-out. This allowed Normalised Difference Vegetation Index (NDVI) values to be related to leaf damage values in order to determine the health of the plants. This study demonstrates that as technology continues to advance, UAV components continually decrease in size, thus allowing much more compact remote sensing UAVs to be developed.

Daniel *et al.* [24] investigates the implementation of remote sensing UAVs into the public network infrastructure to enable civilian security operation. It is explained that installing Air-to-Ground (A2G) links on available cellular networks will enable high coverage for UAV operates, whilst being of low cost. This also ensures frequencies are utilized that are available. This will ultimately enable security companies to utilize the public cellular network to operate remote sensing UAVs within any area to perform security operations. This paper illustrates that remote sensing UAVs can be interfaced with available public cellular networks to be operable where required.

Gu *et al.* [25] implemented air quality sensors onto a UAV with integrated components that is available off the shelf. A S550 hexacopter airframe was used as the aerial platform for the UAV. Particulate Matter of 2.5 micrometres of smaller ($PM_{2.5}$) concentrations and GPS readings were recorded at various regions, including high traffic and low traffic areas. It was determined that $PM_{2.5}$ concentrations increased when near roadways and decreased as the UAV moved away from roads. This investigation illustrates that air quality readings can be recorded and mapped to specific GPS coordinates.
The papers investigated above demonstrates the vast

applications of remote sensing capabilities. Ranging from fixed wing to multi-rotor solutions, air quality sensing can be integrated on multiple platforms. Research also shows that placement of the air quality sensors is crucial to recording valuable and accurate data. Further research and a selection procedure were commenced in order to select the most appropriate air quality sensor for the specific application.

III. SYSTEM ARCHITECTURE

Illustrated in Figure 1 below, the system architecture diagram captures the crucial power, data and pulse width modulation (PWM) lines to corresponding onboard components.

The battery supplies the integrated Power Distribution Board (PDB) through the tracks of the PCB. The power supply is distributed accordingly to power the ESC's, Autopilot (Pixfalcon) and the Raspberry Pi Zero (Figure 2). The autopilot subsequently provides the GPS, pulse position modulation (PPM) module and receiver with the required voltages. PWM signals are transmitted between from RC receiver to the Autopilot and relayed to the ESC's to reflect the desired output. Data signals are transferred from the Autopilot to the GPS and Telemetry. The microprocessor communicates data from the sensors to the Autopilot, then to the Telemetry/Data Link to be transmitted to the ground control station (GCS).
(Ground ⟵ Control ⟵ Station).

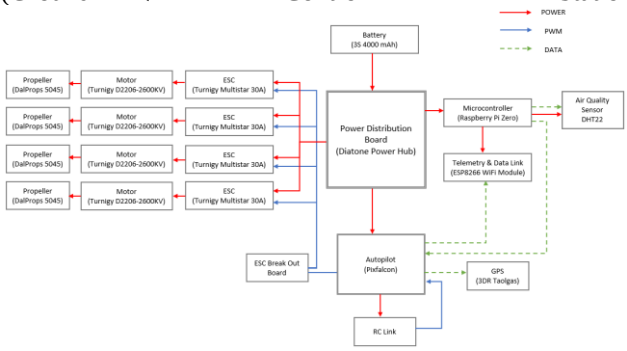

Figure 1. System Architecture Diagram

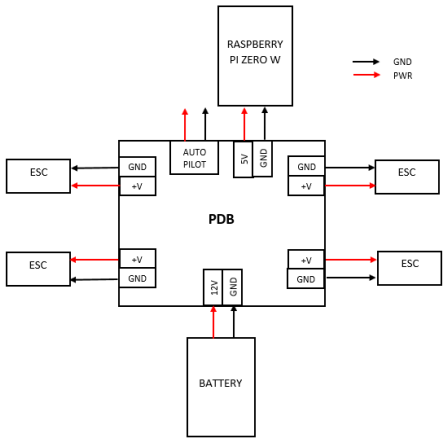

Figure 2. PDB Schematic Diagram

IV. UAV DESIGN

A. *Airframe Design – Initial Design Concepts*

An initial design of the UAV was developed by Mossaddek *et al.*, which consisted of a simplistic box like design, where the rotor arms collapse into a cavity between the top and bottom plates of the UAV chassis [16]. This project allowed the design to be further developed and altered to accommodate design features such as propeller protection.
The initial design phase consisted of formulating various designs ideas acquired from current UAV designs available on the market. In accordance with the project scope, four foldable UAV configurations we considered as inspiration to develop a more rugged UAV design.

Zakaria [17] suggested implementing a PCB would drastically decrease space accommodated by wires and connectors [17]. A PCB design concept was developed. This PCB aimed to mitigate the wired connections running from the battery, to the PDB and from the PDB to the ESC's and additionally to other required subsystems. Subsequently, the PCB will decrease the overall size of the UAV.

B. *Airframe Design – Detailed Design*

The design was progressed to house the subsystems, (Figure 3) illustrates the design.

Figure 3. 3D CAD Detailed UAV Design

Some refinements include; decreasing the overall size of the UAV to meet the 3D printers maximum printable bed size. Altering the shape of the UAV and incorporating a landing gear. Furthermore, the rotor arms were split into four individual arms, thus allowing complete coverage of the propellers. This additionally allowed further freedom to increase the size of the airframe as desired.

From the initial PCB design, a detailed design was developed through utilizing the software platform 'KiCAD'. KiCAD enabled the PCB to be carefully designed to accommodate the shape and size of the UAV. With various design features, KiCAD enabled the PCB to be visualized in 3D. Gerber and drill files were generated and uploaded to 'JLC PCB', a company situated in (Shenzen, China), to manufacture the PCB. The Gerber files describe the images on the PCB, such as; solder mask, copper layers and legend. The drill files describe where the through hole pads are to be drilled. The sole purpose of the PCB is to minimize the wired connections, thus enabling more reliable connections.

Additionally, the PCB mitigates unnecessary wire clutter and allows the UAV to become more compact.

Upon achieving the desired design with the modelling software 'Solid Works', STL (Standard Triangle Language) files were generated for each UAV part. The parts were processed using 'Cura', an open source slicing platform for 3D printing. Following the processing of the parts, the generated gcodes were sent to the Queensland University of Technology (QUT) Additive Manufacturing Team to be printed. Significant amount of supporting structures for the parts were required to be removed for assembly. Aforementioned, numerous design flaws were encountered once the first prototype was manufactured. The first prototype enabled the design to be further refined and developed to mitigate any highlighted issues and implement additional design features. Some of these added features include; a Velcro strap mount for the battery, improved landing gear design, and enhanced folding mechanisms.

C. Material Testing – ABS vs. PET-Glycol (PETG)

Tensile tests were conducted in order to compare the tensile strength and mechanical properties of the material to be utilized for the UAV. Test specimens of PETG and ABS were printed at 20% infill. Utilizing an Instron machine, the test specimens were placed in the machines grips and tightened. As the grips started pulling away from each other, data was recorded for each specimen. Figure 4 and Figure 5 depict the break for each specimen.

Figure 4. ABS Specimen

Figure 5. PETG Specimen

Both specimens fractured at the critical area, where an abrupt change in area is present. The tensile data was translated into 'Stress-Strain' Curves to visually understand the experimental data in a more valuable manner. Figure 6 describes the relationship between the ABS and PETG specimens. As shown in the figure, both materials have a similar performance, with PETG (blue) having more endurance across the loads than ABS (orange).

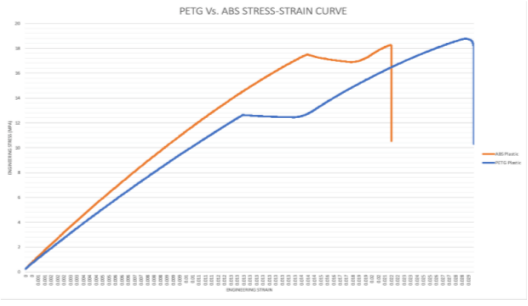

Figure 6. PETG (Blue) vs. ABS (Orange) Stress-Strain Curve

After careful analysis of the data, both materials followed a similar linear trajectory, accommodated with a drip in the centre of the line. The sudden change in the data represents the section along the test where the extensometer was removed, causing a change in the results. According to the tensile results, the calculated tensile strength of ABS plastic is approximately 16.89 MPa and for PETG a recorded tensile strength of 13.45 MPa. With ABS demonstrating a higher tensile strength, PETG experienced more displacement. The tensile test concludes that PETG is approximately equally as strong as ABS, with improved elasticity. This property makes it more desirable for UAV construction than ABS.

V. AIR QUALITY SENSING SYSTEM DESIGN

Zakaria [17] performed a detailed trade study to determine a suitable air quality sensor. The trade study investigation analysed various criteria based on the previous UAV design developed by Mossadek *et al.* [16]. The highlighted criteria the sensors were evaluated against consisted of; Power consumption, size of sensor, accuracy of measurements, Responsiveness, Cost and Operating Conditions.

The three sensors evaluated against the selected criterion mentioned above were; DHT22 [18], DS18B20 and LM35DT.

TABLE I. SENSOR SELECTION CRITERION MATRIX

Sensor Type	**DHT22**	**DS18B20**	**LM35DT**
Power Consumption	< 9mW	< 7.5mW	15 mW
Sensor Size (mm)	15.7x7.7x27	22x32	10x4.6x9
Accuracy of Measurements	Humidity: ± 2% RH Temp: ± 0.5 *C	Temp: ± 0.5 *C	Temp: ± 0.75 *C
Responsiveness	2 secs	1.5 secs	N/A
Cost	$10.00	$6.00	$7.00
Operating Conditions	0-100% RH -40 ~ 80*C	-55 ~ 125*C	0 to 100 *C

Based on the trade study analysis conducted by Zakaria, it was concluded that the DHT22 temperature and humidity sensor is adequate for the UAV design based on the selected criterion.

A. Sensor Operation – DHT22 Temperature and Humidity Sensor

The sensor comprises of a Negative Temperature Coefficient thermistor (NTC Temperature Sensor), humidity sensing element and an Integrating Circuit (IC) [19]. Humidity is measured as the conductivity of the moisture substrate fluctuates. Temperature is recorded as the temperature of the resistor alters its resistiveness.

The DHT22 sensor consist of four pins, VCC+, GND, a data pin and a 'not connected' pin. A resistive component of approximately 5k Ohms - 10k Ohms is necessary to enable the data line to remain in a communicative state between the sensor and microprocessor. A schematic of the sensor and microprocessor can be seen below in Figure 7;

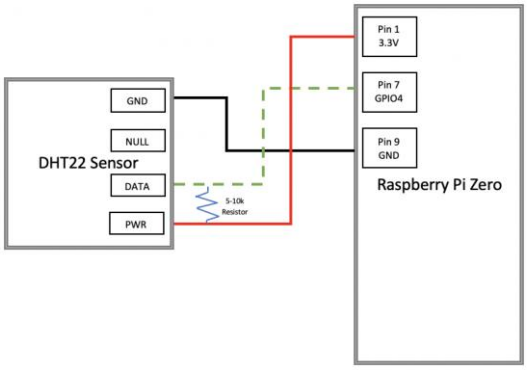

Figure 7. DHT22 Sensor Schematic Diagram

As per the System Architecture Diagram in Figure 2, the DHT22 sensor is powered by the Raspberry microcontroller. The microcontroller is subsequently powered via the PDB. The collected data is communicated from the sensor via the data line into the general-purpose input/output 7 (GPIO) of the Raspberry Pi, as per Figure 7. Aforementioned, a 4.7k (pull-up) resistor is situated between the power and data lines in order to enable the data line to remain within a high state. This is due to data signals being transmitted as either high (1's) or low (0's). The resistor aims to keep the data line high, locked in a high state, mitigating the possibility of a floating data line.

From the microcontroller, the data is communicated to the Ground Control Station (GCS) via the WIFI module. Simultaneously, the RC link communicates to the GCS to navigate the UAV through the planned waypoints. Figure 8 below illustrates the Air Quality subsystem architecture.

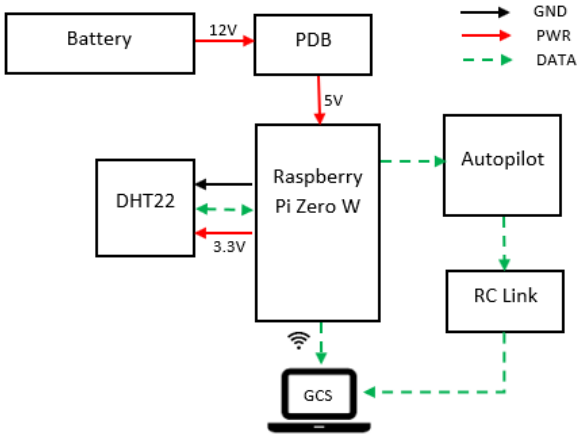

Figure 8. Air Quality Sensor Architecture

B. Final Design

The enhanced design encapsulates a completely independent rotor arm system, while providing full protection for the propeller blades. The ESC placement was adopted from the previous design [16] allowing them to fit in the rotor arms. The top and bottom mounting plate designs are sculpted around the designed PCB and PDB. With the bottom plate having holes to reticulate the power and signal wire to and from the motors. Additionally, a long cavity cut was done on the top plate to allow wires to reticulate to the other onboard subsystems mounted on the top plate. The cavity allows wires to pass through, while still enabling components to be mounted.

The designed foldability mechanism for the rotor arms allow for a compact design. A locking mechanism was developed that involves a spring that snaps the arm into position.
The system uses the same components from the previous design, such as; motors, propellers, PDB, Autopilot, GPS and Raspberry Pi, all the components were integrated onto the new 3D printed design. These components were used again as they have proven to be successful from our previous work [19, 20]. Secure bullet pin connectors, heat shrink, and grommet plugs were implemented to protect the bare wires from moisture and dust. Recent design alterations to improve the functionality and durability of the UAV were procured prior to the manufacturing of the final design. These design decisions include; improved and strengthened landing gear design, additional wire reticulation cavities in the airframe and a canopy redesign to house more hardware components and subsystems.

TABLE II. UAV PARTS PRINTING SUMMARY

Part	**Printing Time**	**Material Consumption (PET) (grams)**
Base and Top Plate	18hrs 15min	39.88 g
Rotor Arms (x4)	40hrs 36min	111.52 g
Canopy	19hrs 34min	38.7 g
Total	78hrs 25min	190.1 g

Based on the gcodes (preparatory codes) generated by the open source slicing platform Cura, the information of each model was captured in Table 2 above. The Lulzbot TAZ 5 printer was utilized to manufacture the airframe parts. Numerous design changes were performed from the initial design. ultimately affecting the printing duration as material usage decreased to reduce the weight of the UAV.

Once all the parts were processed and printed utilizing the QUT Additive Manufacturing services, the UAV was constructed. Minor modifications were required to ensure the parts integrated seamlessly with one another. Filament debris

also required removing to ensure a smooth finish on the parts surfaces. Figure 9 displays the CAD model of the fully integrated UAV.

Figure 9. Final CAD UAV Model and Final Fully Integrated 3D Printed UAV

The final UAV design virtually mirrors the CAD model, as expected. This demonstrates that CAD modelling is a crucial component of design, allowing users to visualize and detect conflicts between parts prior to production. Smaller conflicts can hardly be seen visually, thus producing a prototype is fundamental to determine the functionality and practicality of the design.

VI. TESTING

A. Air Quality Sensing – Subsystem Testing and Analysis

The DHT22 temperature and humidity sensor is connected via three pin connections (Figure 7). Physical pin one provides the DHT22 sensor with a 3.3V power supply in order to operate. The sensor is grounded through physical pin six. The collected data is transmitted through physical pin seven or GPIO4 [20].

In order to enable the Raspberry Pi Zero W to communicate to the sensor and relay the recorded data back to the GCS, the latest Raspbian (Debian-based) computer operating system was flashed onto the SD card. A static IP address was required to be initialised within the operating system to enable it to communicate with the GCS. The raspberry pi was configured to enable remote data access using SSH (Secure Shell). Running a python script (sensors.py) recorded temperature and humidity readings with date and time stamps. Figure 10 below demonstrates the data recorded by the DHT22 sensor and displayed on the GCS in Terminal.

Date	***Time***	***Temp (*C)***	***Humidity (%)***
10/19/19	***15:05:00***	***24.3***	***67.8%***
10/19/19	***15:05:00***	***24.2***	***67.8%***
10/19/19	***15:05:00***	***24.2***	***67.7%***
10/19/19	***15:05:00***	***24.2***	***67.7%***
10/19/19	***15:05:00***	***24.2***	***67.7%***
10/19/19	***15:05:00***	***24.2***	***67.6%***
10/19/19	***15:05:00***	***24.2***	***67.5%***
10/19/19	***15:05:00***	***24.2***	***67.6%***
10/19/19	***15:05:00***	***24.2***	***67.6%***
10/19/19	***15:05:00***	***24.2***	***67.6%***
10/19/19	***15:05:00***	***24.2***	***67.6%***
10/19/19	***15:05:00***	***24.2***	***67.5%***
10/19/19	***15:05:00***	***24.2***	***67.5%***
10/19/19	***15:05:00***	***24.2***	***67.4%***
10/19/19	***15:05:00***	***24.2***	***67.3%***
10/19/19	***15:05:00***	***24.2***	***67.3%***
10/19/19	***15:05:00***	***24.2***	***67.3%***
10/19/19	***15:05:00***	***24.2***	***67.3%***
10/19/19	***15:05:00***	***24.2***	***67.3%***
10/19/19	***15:05:00***	***24.2***	***67.0%***
10/19/19	***15:05:00***	***24.2***	***67.0%***
10/19/19	***15:05:00***	***24.2***	***67.0%***
10/19/19	***15:05:00***	***24.2***	***67.0%***
10/19/19	***15:05:00***	***24.2***	***67.2%***
10/19/19	***15:05:00***	***24.2***	***67.1%***
10/19/19	***15:05:00***	***24.2***	***67.0%***
10/19/19	***15:05:00***	***24.2***	***67.1%***
10/19/19	***15:05:00***	***24.2***	***67.1%***

Figure 10. Air Quality Sensor Readings

The sensors.py script was further developed to store the temperature and humidity readings as a csv file. The data in the .csv excel file is then translated into a more useful format such as plots.

B. Air Quality Sensing – Sensor Placement

Placement of the DHT22 air quality sensors is crucial to acquire accurate temperature and humidity readings of the surrounding environment. Various onboard subsystems required consideration to mitigate factors such as; heat dissipation from hardware components, and downwash produced by the propellers.

After careful analysis of the UAVs airframe, on-board subsystems, and their corresponding locations, it was decided that mounting the DHT22 sensor underneath the UAV on the base plate, suspended by an adjustably platform provided the most accurate temperature and humidity readings shown in Figure 11. Enabling the sensor to be rotated into a desired direction is crucial, as this can increase the quality of the sensor readings, through mitigating sources of heat and/or wind onto the sensor. The suspended mount also enables the sensors to be completely removed from any parent surfaces of the airframe that is prone to heating up. Figure 12 below shows the designed DHTT22 sensors mount for the airframe.

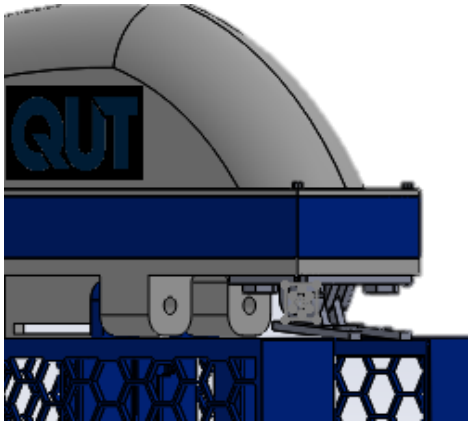

Figure 11. DHT22 Sensor

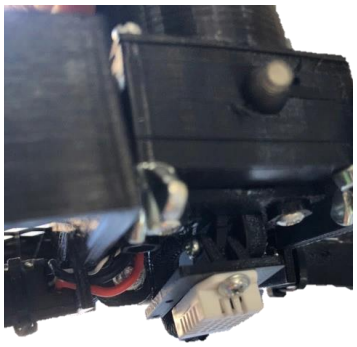

Figure 12. Physical DHT22 Sensor Mount

C. Recycled 3D Printed UAV – Design and Assembly

From the detailed design and prototyping phases, the final design and assembly of the UAV was achieved. The initial and detailed design stages of the project enabled the final design to reflect a well-integrated and successfully functioning product. Through implementing an integrated PCB PDB into the design of the UAV, wiring clutter was mitigated, providing a more compact and seamless UAV design. Figure 13 below depicts the UAV with all the required componentry.

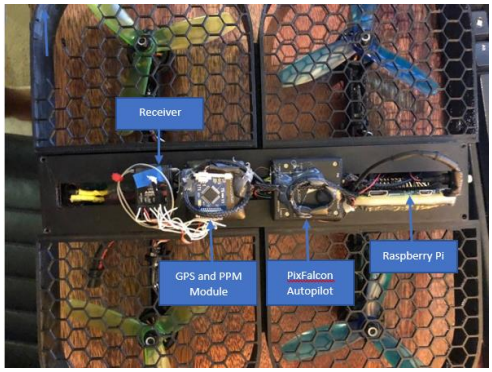

Figure 13. Physical DHT22 Sensor Mount

D. Indoor Flight Test – Manual Flight

Once the UAV was constructed and all the required componentry was assembled onto the airframe, manual manned flight tests were conducted within a safe netted space. This is a crucial step in ensuring the UAV functions are predicted prior to progressing to the autonomous flight stage. Various indoor manned flights were conducted, altering the PID (Proportional, Integral and Derivative) gain values to achieve the best possible response from the UAV.

The UAV was controlled utilizing a Spektrum DX6i transmitter and receiver. The receiver was linked to a PPM encoder, thus enabling the PWM input signals from the RC transmitter to be converted to a single PPM signal.

Once it was established that the UAV was able to successfully operate, the air quality sensor was integrated. Power was sourced by soldering a micro-USB onto the ground output and 5V output terminals on the Power Distribution Board (PDB). The Raspberry Pi Zero W was securely fixed to the top mounting plate of the UAV, and the sensor to the underside of the UAV. The UAV was then placed in the centre of the flight test zone. The props and battery were secured and plugged in. Then the UAV was armed by pressing and holding the safety switch until the arm sound was initialised. Once the UAV was operable, the raspberry pi was ssh'd into and the sensor code was executed to commence recoding temperature and humidity readings. Once the sensor started recording data, the throttle was increased to take-off and get the UAV in the air. The throttle was increased to 50% in order to get the UAV to hover. The UAV was then carefully maneuvered around the designated area, increase and decreasing the throttle, rotating and moving from left to right backwards and forwards. Depicted in Figure 14 below, is the recorded temperature and humidity data during the indoor flight test at hover.

Furthermore, additional indoor flight tests were conducted until the UAV was adequately responding the input controls. During the indoor flight tests, it was concluded that the locking mechanisms was not secure and strong enough to withstand the vibrations created by the motors, thus causing the UAV to be unstable and experiences numerous oscillations from the motors. The rotor arms were redesigned to allow the two separate arms to slide lock into one another, thus reinforcing the entire arm. The design refinement can be seen below in Figure 15;

*Temp (*C)*	*Humidity (%)*
26.1	*60.4%*
25.8	*60.0%*
25.7	*61.6%*
25.6	*61.4%*
25.5	*60.9%*
25.5	*61.4%*
25.5	*61.5%*
25.5	*61.6%*
25.5	*61.5%*
25.4	*61.5%*
25.4	*62.0%*
25.4	*62.2%*
25.4	*62.6%*
25.4	*63.4%*
25.3	*70.8%*
25.1	*70.5%*
25	*68.7%*
24.9	*68.9%*
24.8	*68.4%*
24.8	*68.9%*
24.8	*69.3%*
24.8	*69.5%*
24.8	*69.8%*
24.7	*69.9%*
24.7	*70.6%*
24.7	*70.7%*
24.7	*69.5%*
24.6	*69.5%*

Figure 14. Indoor Flight Test Sensor Data

Figure 15. Sliding Lock Mechanism.

E. Outdoor Flight Test – Manual Flight

After successful indoor manual manned flight tests, outdoor manual manned flight tests were conducted. The outdoor flight tests were carried out on an acreage near Clear Mountain. The 'OpenSky' mobile app was utilized to ensure the Clear Mountain region, Queensland, Australia was deemed suitable and safe to operate a UAV.

Figure 16. Satellite Location of Flight Area

After ensuring it was safe and legal to fly the UAV in the outdoor designated area, the UAV was setup, and the sensor was initialized. The UAV was flown outside, allowing greater altitudes to be achieved, and ultimately test the UAVs capabilities. Temperature and Humidity readings were recorded during the outdoor flight tests. This was a crucial phase, as this demonstrated that the UAV can be operated outdoors within uncontrolled environments. Figure 17 below depicts the UAV flying outdoors

Figure 17. Manual Manned Outdoor Flight Test.

Figure 18 reflects the Ground Control Station (GCS) capturing temperature and humidity readings during one of the outdoor flight tests. It was noted that the Raspberry Pi Zero W only has a WIFI range of approx. 8m. The python script was adjusted to automatically write the recorded values to an excel file, thus allowing the data to be captured and

directly analysed after each flight test.

*Temp (*C)*	*Humidity (%)*
32.3	*35.9%*
29.8	*37.2%*
29.5	*37.1%*
29.5	*37.2%*
29.5	*37.2%*
29.4	*37.3%*
29.4	*37.4%*
29.4	*38.1%*
29.2	*38.4%*
28.9	*38.5%*
28.8	*38.6%*
28.8	*38.6%*
28.7	*38.7%*
28.7	*38.8%*
28.7	*38.8%*
28.6	*39.5%*
28	*39.9%*
27.7	*40.2%*
27.3	*40.2%*
27.2	*40.2%*

Figure 18. GCS and Sensor Results

F. Outdoor Flight Test – Autonomous Flight

After subsequent manual outdoor flight tests, it was proven that the designed concept was feasible. Thus, the UAV was enabled to commence autonomous flight. The UAV was prepared for autonomous flight, by adding a GPS module and telemetry link to permit communication between the GCS and UAV. Additionally, the UAVs sensors required recalibration to ensure it is equivalent to the GPS. QGround Control was utilized as the designated GCS, and a waypoint flight plan was created. Four waypoints were added to the mission flight path, and the desired altitudes were specified at each waypoint. Once the flight path was completed, it was loaded onto the autopilot. Once the UAV commenced onto the flightpath, the sensor was simultaneously activated in order to commence temperature and humidity data collection. Figure 19 below depicts the view of the GCS;

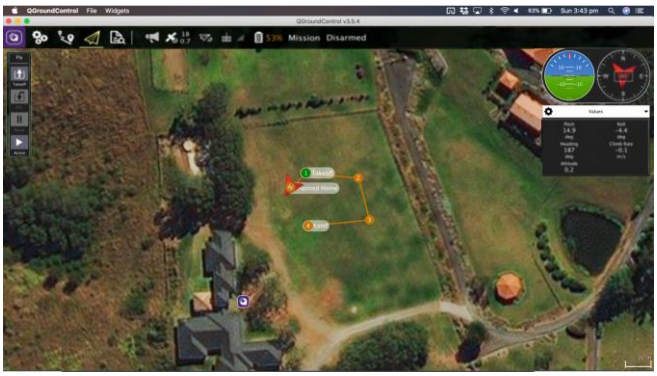

Figure 19. Outdoor Autonomous Waypoint Flight taking Sensor Readings

The sensor readings were communicated to the GCS via the ssh command executed in terminal. It was established that the raspberry pi only has a small Wi-Fi range, thus the python script was modified to store the recorded readings into a .csv file. This file can then be opened by utilizing excel to view the recorded data.

VII. CONCLUSION AND FUTURE WORK

The main focus of this paper was to design and develop a foldable recycled 3D printed UAV with a remote sensing capability. This paper successfully executed and provided supporting evidence of a feasible solution. Simultaneously, this paper also provides practical evidence of a UAV being manufactured from recycled PETG plastic, mitigating the significant amount of plastic waste, while fuelling the ever-growing demand of UAVs. This paper set out to design, manufacture and test a foldable 3D printed UAV, that is printed from a recycled plastic filament. The main features of the UAV consist of; foldable arms, fully encaged/covered propellers, and air quality sensing. The UAV successfully recorded temperature and humidity readings during the manned flight stage. The data was analysed, and it was concluded that the captured temperature and humidity readings were reasonably accurate measurements. This was conducted by comparing temperature and humidity data from the Bureau of Meteorology for the test location [26]. Furthermore, the air quality sensing was extended onto the autonomous platform, successfully capturing data readings.

Thus, it can be concluded that with sound theoretical and experimental confirmation that, constructing a UAV from 3D printed recycled plastic filament (PETG) with an integrated DHT22 air quality sensor is a feasible solution to mitigating the vast amount of plastic waste. This solution can be further developed due to the significantly positive impact it poses to the environment and the growing UAV industry. Furthermore, the UAV can be developed to house other onboard sensors and/or cameras to perform additional remote sensing tasks.

One recommendation that must strongly be considered is to further investigate solutions to enable Wi-Fi ranges to be extended. This will allow live data to be transmitted to the Ground Control Station, thus allowing the UAV to explore areas more remote.

Extending the ability of the Printed Circuit Board to house other onboard components, sensors and even the autopilot itself will significantly reduce the size of the UAV.

Further studies can be conducted into utilising the UAV with protected propellers in more remote areas. Additionally, further attachments can be developed such as open rotor arms, that can easily be interfaced with the current design if protected propeller arms are not required. Also, further development of the PCB can be explored to enable more subsystems to be integrated into the design.

ACKNOWLEDGEMENTS

The authors of this paper thank the Science and Engineering Faculty at QUT, and the Additive Manufacturing Team for financial support and advise throughout the duration of the project. Additionally, the authors thank Kye Morton and Abdul Amir Bin Zakaria for providing technical support and advise.

REFERENCES

[1] Valavanis K.P., Vachtsevanos G.J. (2015) UAV Design Principles: Introduction. In: Valavanis K., Vachtsevanos G. (eds) Handbook of Unmanned Aerial Vehicles. Springer, Dordrecht

[2] S. Zermani, C. Dezan and R. Euler (2017) "Embedded decision making for UAV missions," 2017 6th Mediterranean Conference on Embedded Computing (MECO), Bar, 2017, pp. 1-4.

[3] D. Lee, L. Gonzalez, K. Srinivas, D. Auld and K. Wong (2006) "Aerodynamic/RCS Shape Optimisation of Unmanned Aerial Vehicles Using Hierarchical Asynchronous Parallel Evolutionary Algorithms" 2006 24th AIAA Conference on Applied Aerodynamics, San Francisco, California.

[4] S. Ward, J. Hensler, B. Alsalam, L.F. Gonzalez. "Autonomous UAVs wildlife detection using thermal imaging, predictive navigation and computer vision. In Proceedings of the 2016 IEEE Aerospace Conference, Big Sky, MT, USA, 5–12 March 2016.

[5] M. Alvarado, F. Gonzalez, P. Erskine, D. Cliff. and D. Heuff, "A Methodology to Monitor Airborne PM10 Dust Particles Using a Small Unmanned Aerial Vehicle, Sensors, 17, 343, https://doi.org/10.3390/s17020343, 2017.

[6] L. González, E. Whitney, K. Srinivas and J. Périaux (2004) "Multidisciplinary Aircraft Design and Optimisation Using a Robust Evolutionary Technique with Variable Fidelity Models" 2004 10th AIAA/ISSMO Multidisciplinary Analysis and Optimisation Conference, Albany, New York.

[7] W. Al-Sabban, L. Gonzalez, R. Smith and G. Wyeth (2012) "Wind-energy based path planning for electric unmanned aerial vehicles using Markov Decision Processes" 2012 In Proceedings of the IEEE/RSJ International Conference on Intelligent Robots and Systems, IEEE, Vilamoura, Algarve.

[8] A. Chapman, "Types of Drones: Multi-Rotor vs Fixed-Wing vs Single Rotor vs Hybrid VTOL - AUAV", AUAV, 2019. [Online]. Available: https://www.auav.com.au/articles/drone-types/.

[9] "A Guide to Electronic Speed Controllers", Modelflight.com.au, 2019. [Online]. Available: https://www.modelflight.com.au/blog/electronic-speed-controllers.

[10] "Everything You Need to Know About Electronic Speed Controllers (ESC) - HobbyKing News", Hobbyking, 2019. [Online]. Available: https://hobbyking.com/en_us/news/everything-need-know-electronic-speed-controllers-esc?___store=en_us.

[11] "Additive Manufacturing Definition: What is Additive Manufacturing? | SPI Lasers", SPI Lasers, 2019. [Online]. Available: https://www.spilasers.com/application-additive-manufacturing/additive-manufacturing-a-definition/.

[12] "3D Printing Technologies and Techniques", Sculpteo, 2019. [Online]. Available: https://www.sculpteo.com/en/3d-printing/3d-printing-technologies/.

[13] "STL File Format (3D Printing) – Simply Explained | All3DP", All3DP, 2019. [Online]. Available: https://all3dp.com/what-is-stl-file-format-extension-3d-printing/.

[14] "3D Printing STL files: A step-by-step guide | 3D Hubs", 3D Hubs, 2019. [Online]. Available: https://www.3dhubs.com/knowledge-base/3d-printing-stl-files-step-step-guide/.

[15] "3D Printer Filament Comparison | MatterHackers", MatterHackers, 2019. [Online]. Available: https://www.matterhackers.com/3d-printer-filament-compare.

[16] A. Mosaddek, Hrushi K. & F. Gonzalez (2018) "Design and Testing of a Recycled 3D Printed and Foldable Unmanned Aerial Vehicle for Remote Sensing." In Johansen, T A & Theilliol, D (Eds.) *Proceedings of the 2018 International Conference on Unmanned Aircraft Systems (ICUAS 2018):* IEEE, United States of America, pp. 1207-1216.

[17] A. Zakaria, F. Gonzalez, "Design and Testing of a Recycled 3D Printed Foldable Advance Unmanned Aerial Vehicle for Air Quality Sensing.", QUT,2019.

[18] Cdn-shop.adafruit.com, 2019. [Online]. Available: https://cdn-shop.adafruit.com/datasheets/DHT22.pdf.

[19] "DHT11 & DHT22 Sensor Temperature and Humidity Tutorial", HowToMechatronics, 2019. [Online]. Available: https://howtomechatronics.com/tutorials/arduino/dht11-dht22-sensors-temperature-and-humidity-tutorial-using-arduino/.

[20] G. W, D. Desyllas, D. Desyllas and M. W, "GPIO Pinout Orientation RaspberyPi Zero W", Raspberry Pi Stack Exchange, 2019. [Online]. Available: https://raspberrypi.stackexchange.com/questions/83610/gpio-pinout-orientation-raspberypi-zero-w.

[21] "Remote Sensing", Mdpi.com, 2019. [Online]. Available: https://www.mdpi.com/journal/remotesensing/special_issues/remotesensing_drone.

[22] U. Niethammer, M. James, S. Rothmund, J. Travelletti and M. Joswig (2012) "UAV-based remote sensing of the Super-Sauze landslide: Evaluation and results" Engineering Geology, V. 128, Pages 2-11.

[23] S. Nebiker, A. Annen, M. Scherrer and D. Oesch, A light-weight multispectral sensor for micro UAV -opportunities for very high resolution airborne remote sensing 2008, pp. 1193-1199.

[24] K. Daniel and C. Wetfield, Using Public Network Infrastructures for UAV Remote Sensing in Civilian Security Operations. 2011.

[25] Q. Gu, D. Michanowicz and C. Jia, "Developing a Modular Unmanned Aerial Vehicle (UAV) Platform for Air Pollution Profiling" Sensors 2018.

[26] 'Redcliffe, Qld - October 2019 - Daily Weather Observations'. Available:http://www.bom.gov.au/climate/dwo/201910/html/IDCJDW4099.201910.shtml